Theoretical Study of Structures, Energies, and Vibrational Spectra of the Imidazole−Imidazolium System

Wiktor Tatara and Marek J. Wójcik*

Faculty of Chemistry, Jagiellonian University, 30-060 Kraków, Ingardena 3, Poland

Jan Lindgren

Ångstrom Laboratory, Department of Materials Chemistry, Uppsala University, Box 538, SE-751 21 Uppsala, Sweden

Michael Probst

Institut fur Ionenphysik, Leopold Franzens Universitat Innsbruck, A-6020 Innsbruck, Austria

Received: January 16, 2003; In Final Form: May 15, 2003

Energies, structures, vibrational spectra, and proton transfer in the imidazole−imidazolium complex have been studied by B3LYP/6-311++G** method. This complex is a strongly hydrogen-bonded system with a low energy barrier for the proton-transfer reaction and the rotation of the imidazolium ion along the axis of the complex. The calculations predict that a classical motion of the proton between the two molecules in the complex is allowed. A strong influence of the complex formation on the vibrational spectra has been observed in the N−H stretching mode and in the fingerprint region. Several modes in the fingerprint region have been shown to give suitable indicator bands for complex formation detection in polymer electrolytes where imidazole and imidazolium ions have been added.

Introduction

Highly efficient energy production from renewable sources with practically no pollutant emission is a goal of many teams working in either universities or industries. Fuel cell technology is expected to become one of the key technologies of the 21st century both for stationary applications such as block power stations and in applications such as personal vehicles, trucks, buses, and locomotives, because the fuel utilization in fuel cell engines is markedly higher than in combustion engines. Among many kinds of fuel cells polymer electrolyte fuel cells (PEFC) have attracted much interest recently.[1] In these cells a polymer electrolyte membrane acts as a medium for proton conductivity. Traditionally, the membrane used is a hydrated perfluorosulfonic polymer such as Nafion, where the proton transfer occurs through a Grotthuss-type mechanism involving hydronium ions, H_3O^+, and water molecules.

It has been suggested by Kreuer et al.,[2,3] that the use of heterocycles such as pyrazole and imidazole could be an interesting alternative to a water-based system. In this case the protons should primarily be transferred from the sulfonic groups to the heterocycle and charge carriers $(C_3H_3NH_2)^+$ are formed. There should then be a possibility for proton jumps between, e.g., imidazole and imidazolium ions resembling the case for water and hydronium ions. It was shown that high protonic conductivity could be obtained, also at higher temperatures, for imidazole or pyrazole in sulfonated polyetherketone membranes. Sun et al.[4] used water-free Nafion 117 membranes that were swollen by imidazole−imidazolium salt solutions. Conductivities in the range of 10^{-3} S cm^{-1} at around 100 °C were obtained in that case. A calculation of the mechanism for proton diffusion in imidazole chains containing an excess proton have been performed using ab initio molecular dynamics simulations.[5]

The present work is based on quantum mechanical calculations on the imidazole−imidazolium system. Equilibrium geometries and energies as well as the shape of the potential energy for proton transfer have been calculated. Vibrational spectra for the different constituents have been calculated as an aid for the interpretation of experimental spectra of polymer membranes containing imidazole−imidazolium ions, which will be the subject of a forthcoming work.

Quantum Chemical Calculations

Density functional theory calculations have been performed using the GAUSSIAN 98 programs.[6] Initial structures were determined by the semiempirical AM1 method.[7] Calculations have been carried out for isolated imidazole (Im) and imidazolium (ImH^+) molecules as well as for the hydrogen-bonded imidazolium−imidazole (ImH^+−Im) system. Stable and saddle point structures for proton transfer of the imidazolium−imidazole complex were established at the B3LYP/6-311++G** (DFT) level. We have checked the influence of BSSE using the ghost atoms method.[21,22] The influence on results is negligible. Vibrational frequency calculations were performed at the same level of theory to confirm that the structures were true minima or transition states.

Complex formation energies and energy barriers are defined as follows:

$$E_{\text{bond}} = E(\text{ImH}^+\text{−Im}) - [E(\text{ImH}^+) + E(\text{Im})]$$

$$E_{\text{barrier}} = E(\text{ImH}^+\text{−Im, saddle point}) - E(\text{ImH}^+\text{−Im, stable})$$

* Corresponding author. Fax: +48-12-634-05-15. E-mail address: wojcik@chemia.uj.edu.pl.

10.1021/jp030065z CCC: $25.00
Published on Web 09/09/2003

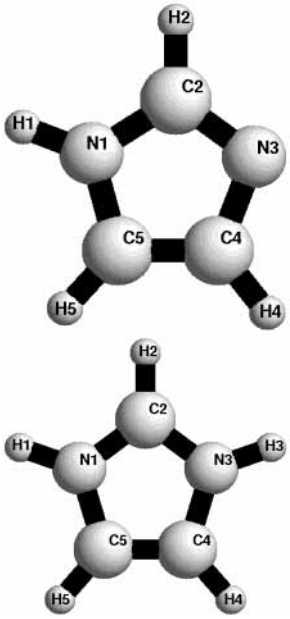

Figure 1. Structure of imidazole (Im) and imidazolium (ImH^+) ion.

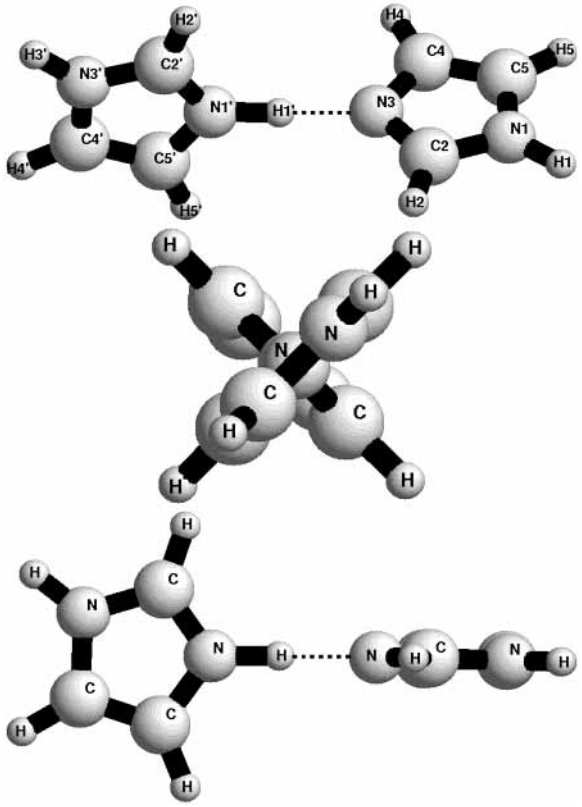

Figure 2. Structure of imidazolium−imidazole complex in stable geometry.

Relaxed potential energy surface (PES) scan calculations were performed at the Becke3Lyp/6-31++G** level for the proton transfer between imidazolium and imidazole molecules and for the rotation of imidazolium along the N−H···N axis. The step size for these calculations was 0.05 Å and 5°, respectively.

Results and Discussion

Structures and Energies. Figures 1−3 present structures of the isolated imidazole (Im) molecule, the imidazolium (ImH^+) ion, and the hydrogen-bonded system (ImH^+−Im) in the energy minimum and at the saddle point for proton transition between ImH^+ and Im. Both Im and ImH^+ are planar molecules with symmetries C_s and C_{2v}, respectively. In Table 1 experimental[8] microwave spectroscopy-deduced and calculated bond lengths of the isolated Im are listed.

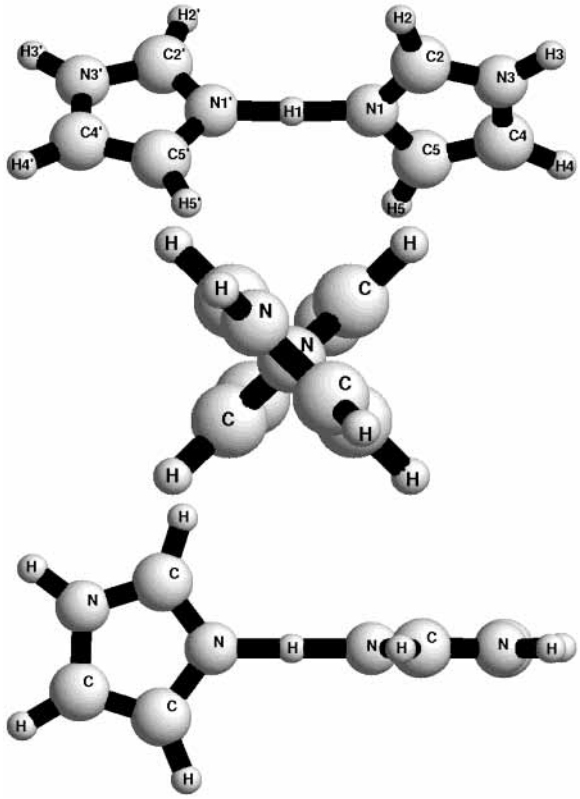

Figure 3. Structure of imidazolium−imidazole complex in saddle point geometry.

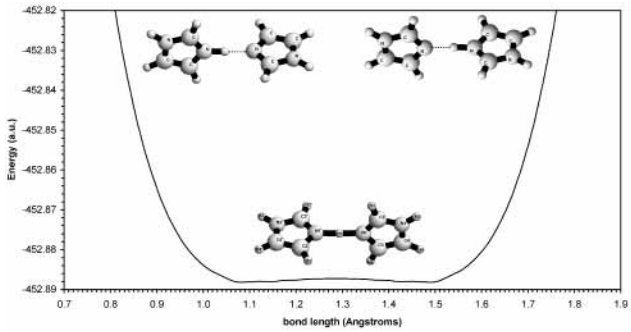

Figure 4. Potential energy shape for proton transfer.

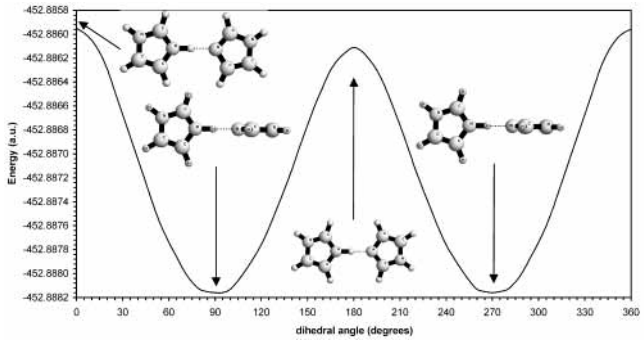

Figure 5. Potential energy shape for rotation of ImH^+ molecule in ImH^+−Im complex.

TABLE 1: Calculated Bond Lengths (Å) and Angles (deg) of Imidazole (Im) and Imidazolium (ImH^+) Isolated and in Imidazolium−Imidazole (ImH^+−Im) System

			ImH^+−Im				ImH^+−Im
molecule	bond	isolated	stable structure	exp stable[8]	angle	isolated	stable structure
Im	N_1C_2	1.367	1.352	1.314	$N_1C_2N_3$	111.5	110.3
	C_2N_3	1.313	1.323	1.364	$C_2N_3C_4$	105.5	106.4
	N_3C_4	1.377	1.382	1.382	$C_2N_1C_5$	107.2	108.2
	N_1C_5	1.380	1.379	1.377	$N_1C_5C_4$	110.6	109.5
	C_4C_5	1.371	1.366	1.364	$N_3C_4C_5$	105.1	105.5
	N_1H_1	1.008	1.010	0.998	$C_2N_1H_1$	126.5	125.8
	C_2H_2	1.079	1.078	1.079	$N_3C_2H_2$	126.0	126.2
	C_4H_4	1.079	1.078	1.078	$N_3C_4H_4$	121.4	122.0
	C_5H_5	1.077	1.076	1.078	$N_1C_5H_5$	122.3	122.5

			ImH^+−Im				ImH^+−Im	
molecule	bond	isolated	stable structure	calc saddle point structure	angle	isolated	stable structure	calc saddle point structure
ImH^+	$N'_1C'_2$	1.334	1.327	1.325	$N'_1C'_2N'_3$	107.1	108.3	109.4
	$C'_2N'_3$	1.334	1.342	1.347	$C'_2N'_1C'_5$	110.0	108.7	107.5
	$N'_3C'_4$	1.383	1.382	1.380	$C'_2N'_3C'_4$	110.0	109.2	108.7
	$N'_1C'_5$	1.383	1.380	1.381	$C'_4C'_5N'_1$	106.5	107.7	108.6
	$C'_4C'_5$	1.360	1.362	1.364	$N'_3C'_4C'_5$	106.5	106.1	105.8
	$N'_1H'_1$	1.013	1.108	1.286	$C'_2N'_1H'_1$	124.5	125.3	126.5
	$N'_3H'_3$	1.013	1.011	1.010	$C'_2N'_3H'_3$	124.5	125.0	125.4
	$C'_2H'_2$	1.078	1.077	1.078	$N'_1C'_2H'_2$	126.5	126.2	126.2
	$C'_4H'_4$	1.077	1.076	1.076	$N'_1C'_5H'_5$	122.4	122.1	122.0
	$C'_5H'_5$	1.077	1.076	1.077	$N'_3C'_4H'_4$	122.4	122.4	122.4
ImH^+−Im	$N_3N'_1$		2.670	2.572	$C_2N_3H'_1$		128.4	126.5
	$N_3H'_1$		1.562	1.286	$C_2N_3N'_1C'_2$		91.4	90.0

TABLE 2: Energies, Bonding Energies, and Proton-Transfer Energy Barriers

	no ZPE (au)	with ZPE (au)
imidazole (au)	−226.2828	−226.2120
imidazolium (au)	−226.6549	−226.5700
ImH^+−Im stable structure (au)	−452.9819	−452.8259
ImH^+−Im saddle point structure (au)	−452.9807	−452.8280
E_{bond} (kJ/mol)	−115.85	−115.43
$E_{barrier}$ (kJ/mol)	3.10	−5.51

TABLE 3: Energies and Energy Barriers from Relaxed PES Calculations

Proton Transfer			
energy			
stable structure (au)		−452.8882	
saddle point structure (au)		−452.8873	
$E_{barrier}$ (kJ/mol)		2.39	
Rotation Along the N−H···N Axis			
dihedral angle $C_2N_3N_1'C_2'$ (deg)	0	90 (270)	180
Energy (au)	−452.8860	−452.8882	−452.8861
$E_{barrier}$ (kJ/mol)	5.80		5.38

The calculated geometry is in good agreement with the experimental one; however, there is some overestimation of the N−H bond and underestimation of the N_3C_4 bond. There is a lack of experimental data for ImH^+. The energy of the ground state of ImH^+ is lower than that of Im (0.3721 au (no ZPE) and 0.3580 au (with ZPE) see Table 2).

In the case of the ImH^+−Im complex the planes of ImH^+ and Im are almost orthogonal to each other (91.4°) in the stable structure and orthogonal in the saddle point structure. The symmetry of the stable structure is C_1. The saddle point structure has C_2 symmetry with the proton situated on the 2-fold axis between the molecules. ImH^+−Im is a strongly hydrogen-bonded complex (Table 2). The absolute value of the bonding energy of the complex is 115.85 kJ/mol (no ZPE) and 115.43 kJ/mol (with ZPE) (see Table 2). There is a small energy barrier (3.10 kJ/mol); however, the ground-state energy adjusted by the zero point energy lies above the energy barrier for the proton transfer (5.51 kJ/mol). This means that, according to the DFT calculations, classical motion of the proton between the two molecules is allowed.

In Table 1 the bond lengths and angles are listed. The hydrogen bond length in the stable structure is 2.670 Å, N_1'−H_1' bond length is 1.108 Å. The increase of the N_1'−H_1' bond length after formation of the ImH^+−Im complex is about 0.095 Å. The bonds involving the heavy atoms show smaller changes (see Table 1). The C−N bond lengths change on the order of 0.005 Å. The bond angles change very little and the largest changes occur for the C−N−C angles for the nitrogens involved in the hydrogen bond. In the case of the geometry of the saddle point, the length of the hydrogen bridge is shorter by 0.098 Å and the distance between the nitrogen atom and hydrogen is 1.286 Å.

Shape of Potential Energies−Proton Transfer and Rotation. Figure 4 shows the shape of the potential energy from the relaxed potential energy surface (PES) scan calculations for the proton-transfer reaction. Table 3 contains data for energies and energy barriers for proton transfer and rotation of ImH^+ along the $N_1'H_1'N_3$ axis. As found before (Table 2), the DFT ground state is located above the energy barrier. The proton-transfer potential energy curve has a broad double well shape with a very small energy barrier. At room temperature the proton can move undisturbed from one side to the other. The potential energy curve for rotation of ImH^+ in the complex has two minima for the identical perpendicular orientations (at 90 and 270°) and two maxima (at 0 and 180°). Due to the specific locations of the nitrogen atoms in the five-membered aromatic rings of Im and ImH^+, the 180°-trans orientation lies lower in energy than the 0°-cis one. Their difference is only 0.43 kJ/mol.

The barrier for proton transfer between ImH^+ and Im has been calculated before,[9] and a value of 38 kJ/mol was obtained for the barrier height. However, no complete geometry optimi-

TABLE 4: Calculated Frequencies (cm^{-1}) of Imidazole

no.	sym	freq	IR int	description[a]
1	A′	3655	59.20	NH str
2	A′	3273	0.97	CH str
3	A′	3245	0.78	CH str
4	A′	3242	4.83	CH str
5	A′	1555	11.98	CC str, XH bip
6	A′	1496	21.87	CC, CN str, CH bip
7	A′	1430	15.91	CC, CN str, NH bip
8	A′	1362	6.56	CN str, CH bip
9	A′	1282	0.40	CN str, CH bip
10	A′	1160	4.91	CN str
11	A′	1145	4.00	XH bip, CN str
12	A′	1092	20.99	XH bip, CN, CC str
13	A′	1073	41.40	CN_1C bip, CH bip
14	A′	945	2.13	CN_3C bip
15	A′	908	6.60	CN_1C bip
16	A″	866	4.97	CH bop
17	A″	808	37.83	CH bop
18	A″	729	43.07	CH bop
19	A″	678	5.88	ring def op
20	A″	640	10.68	ring def op
21	A″	517	97.61	NH bop

[a] str: stretching. bip: bending in plane. bop: bending out of plane. ring def: ring deformation.

TABLE 5: Calculated Frequencies (cm^{-1}) of the Imidazolium Ion

no.	sym	freq	IR int	description[a]
1	A1	3610	28.55	NH str sym
2	A1	3298	17.17	CH str sym
3	A1	3282	54.57	C_1H str
4	A1	1627	52.00	NH bip sym, CC str
5	A1	1467	5.08	CC, CN str, XH bip sym
6	A1	1218	12.44	CN str, XH bip sym
7	A1	1126	2.49	CC str, CH bip sym
8	A1	1113	23.44	CN str, XH bip sym
9	A1	942	0.46	CNC bip, CH bip sym
10	B2	3602	363.65	NH str asym
11	B2	3281	26.14	CH str asym
12	B2	1557	8.68	CH bip
13	B2	1463	15.76	NH bip asym
14	B2	1336	0.28	CH bip asym
15	B2	1195	0.59	CH bip
16	B2	1064	38.12	CN str, CH bip asym
17	B2	922	0.59	CNC bip asym
18	A2	894	0.00	CH bop sym
19	A2	688	0.00	NH bop sym
20	A2	626	0.00	NCCN bop sym
21	B1	863	0.50	CH bop
22	B1	766	91.60	CH bop asym
23	B1	730	170.61	NH bop asym
24	B1	626	53.79	CNC bop asym

[a] sym: symmetrical. asym: antisymmetrical.

zation was done at that time. The proton-transfer properties of imidazole have also been discussed before.[10] In this case the proton transfer from ImH^+ to an ammonia molecule was considered. The minimum energy structure for the system was obtained for $ImH^+\cdots NH_3$ with the proton attached to Im. In the transition state an inter-nitrogen distance of 2.585 Å was found for $Im\cdots H^+\cdots NH_3$, which is quite close to the value (2.572 Å) obtained in the present case for $Im\cdots H^+\cdots Im$. In the case of Im and ammonia two different inter-nitrogen distances were obtained for the other two stationary points along the proton-transfer potential depending on whether the proton was attached to ammonia (2.687 Å) or to imidazole (2.893 Å). The diffusion mechanism of an excess proton in imidazole chains has been studied recently.[5] In that case the proton transfer was found to be coupled to a reorientation step. In one of the chains

TABLE 6: Calculated Frequencies (cm^{-1}) of the ImH^+-Im Complex in the Stable Structure

no.	sym	freq	IR int	center	description[a]
1	A	3638	122.44	IM	N_1H str
2	A	3626	163.46	IMH	$N_3′H_3′$ str
3	A	3296	6.77	IMH	CH str
4	A	3287	3.72	IM	CH str
5	A	3282	27.88	IMH	CH str
6	A	3278	13.29	IMH	CH str
7	A	3263	5.30	IM	CH str
8	A	3259	1.36	IM	CH str
9	A	2049	4812.94	IMH	$N_1′H_1′$ str
10	A	1652	51.51	IMH	NH, CH bip, CC str
11	A	1575	40.65	IM	NH, CH bip, CC str
12	A	1549	23.17	IMH	CN str CH, NH bip
13	A	1537	14.93	IMH	NH bip, CC str
14	A	1520	189.53	IM	CN str, CH bip
15	A	1460	2.19	IMH	NH bip, CC, CN str
16	A	1450	13.91	IM	NH bip, CC, CN str
17	A	1379	20.93	IM	$N_1′H_1′$ bop, CH bip, CN str
18	A	1353	1.71	IMH	CH, NH bip, CN str
19	A	1320	9.03	IM	CH, NH bip, $N_1′H_1′$ bop
20	A	1263	38.19	IM	CH, NH bip, $N_1′H_1′$ bop
21	A	1256	15.21	IMH	CH, NH bip, CN str
22	A	1188	77.48		CN str, CH, NH bip
23	A	1182	26.04		CH, NH bip, CN str
24	A	1142	37.72		CH, NH bip, CN str
25	A	1140	3.77		CH, NH bip, CN str
26	A	1120	22.26	IMH	CH, NH bip
27	A	1117	23.47	IM	CH, NH bip
28	A	1083	83.63	IM	CH, NH bip, CN str
29	A	1069	17.64	IMH	CH, NH bip, CN str
30	A	963	33.14	IM	ring def
31	A	940	15.87	IMH	ring def
32	A	937	18.93	IM	ring def
33	A	885	1.33	IMH	CH bop
34	A	878	1.59	IM	CH bop
35	A	870	251.11	IMH	$C_5N_1C_2$ bip (ring def)
36	A	843	26.56	IMH	CH bop
37	A	830	27.41	IM	CH bop
38	A	764	45.51	IMH	CH bop
39	A	760	42.74	IM	CH bop
40	A	687	48.56	IMH	$N_3′H_3′$ bop
41	A	681	1.62	IM	NH, CH bop
42	A	651	42.21	IM	NH, CH bop
43	A	642	30.85	IMH	NH, CH bop
44	A	620	39.13	IMH	NH, CH bop
45	A	600	73.83	IM	NH, CH bop
46	A	156	84.70		N−H···N str
47	A	150	1.23		rot.
48	A	132	4.78		rot.
49	A	56	4.71		rot.
50	A	53	4.62		rot.
51	A	36	0.72		rot.

the protonic defect induced differing N−N separations in the hydrogen bridge ranging from 2.61 to 2.73 Å, which can be compared to the value 2.670 Å obtained for the minimum energy structure in the present case.

Vibrational Spectra. Tables 4 and 5 contain calculated frequencies of imidazole and the imidazolium ion, and Tables 6 and 7 list calculated frequencies of the ImH^+-Im system in the minimum energy and saddle point structures. The vibrational modes of imidazole have A′ (in plane) or A″ (out of plane) symmetry, and all are Raman and IR active. The assignment of the planar modes of imidazole in the frequency range below 1600 cm^{-1} has been the subject of extensive discussions.[11−18] The assignment proposed here is consistent with that made by Majoube et al.[19] and Sadlej et al.[20] The imidazolium modes, due to the higher point group symmetry (C_{2v}), have either A_1, A_2, B_1, or B_2 character. All modes are Raman active whereas the A_2 (out of plane) modes are inactive in IR. The present

TABLE 7: Calculated Frequencies (cm^{-1}) of the ImH^+−Im System in the Saddle Point Structure

no.	sym	freq	no.	sym	freq
1	A	3632	27	B	*i*796
2	A	3290	28	B	3632
3	A	3272	29	B	3290
4	A	3269	30	B	3272
5	A	1616	31	B	3269
6	A	1551	32	B	1612
7	A	1527	33	B	1535
8	A	1456	34	B	1527
9	A	1353	35	B	1457
10	A	1281	36	B	1353
11	A	1216	37	B	1271
12	A	1151	38	B	1200
13	A	1120	39	B	1141
14	A	1088	40	B	1121
15	A	993	41	B	1079
16	A	940	42	B	1001
17	A	883	43	B	939
18	A	837	44	B	882
19	A	763	45	B	837
20	A	683	46	B	762
21	A	650	47	B	683
22	A	613	48	B	650
23	A	258	49	B	612
24	A	151	50	B	152
25	A	59	51	B	59
26	A	37			

description of the imidazolium ion modes was compared with that published by Majoube et al.,[19] and the only discrepancy found is the symmetry of the modes with numbers 10−17 (Table 7), which we found to be B_2 instead of A_2 in agreement with the result of Sadlej et al.[20]

The formation of the complex strongly influences the vibrational spectra as compared to the ones for the free Im and ImH^+ parts. The symmetry of the ImH^+−Im system is C_1, which makes all modes Raman and IR active. Table 6 presents a set of normal modes of ImH^+−Im calculated at the B3LYP/6-311++G** level. Most of the modes of the complex remain well separated and centered on imidazole or imidazolium. However, the modes numbers 22−25 and 46−51 are combinations of vibrations of both molecules. The former group involves mostly the in-plane bending of the N−H and C−H bonds, whereas the latter group consists of a N−H···N stretching mode (Table 6 mode number 46 with the wavenumber 156 cm^{-1}), and rotational vibrations of the molecules in the complex.

The most affected modes by the hydrogen bond formation are the N−H stretching modes of the ImH^+ molecule. These modes have lost their A_1 and B_2 character and split into two well-separated N−H stretching vibrations. The first N−H mode of ImH^+ (Table 6, mode 2 at 3626 cm^{-1}) has a frequency similar to that in the isolated system (Table 5, mode 1 and 10), whereas the second mode (Table 6, mode 9), which is the N−H stretching vibration of the bond involved in the hydrogen bond formation, has a much lower frequency at 2049 cm^{-1}. These large shifts are the result of the strong hydrogen bond between ImH^+ and Im.

The group of bands (numbers 22−25 in Table 6) are interesting as possible indicator bands for the formation of the ImH^+−Im complex in polymer electrolyte systems where imidazole and imidazolium ions have been added. These bands have contributions from both constituents, and have positions in the spectra where no or only a small overlap by bands from Im and ImH^+ occurs. These bands will be used in a forthcoming work on Raman spectra of some polymer electrolyte systems.

Table 7 shows calculated frequencies of the ImH^+−Im complex in its transition state. Because the point group of the saddle point structure is C_2, the normal modes can be of A or B symmetry. The imaginary mode number 27 shifts the proton from the center of the complex toward one or the other molecule. The presence of the only one imaginary frequency confirms that the structure is a truly saddle point structure.

Conclusions

Our calculations show that the imidazolium−imidazole complex is a strongly hydrogen-bonded system with low-energy barriers for the proton-transfer reaction and the rotation of the imidazolium ion along the axis of the complex. The calculations predict that a classical motion of the proton between the two molecules in the complex is allowed. A strong influence of the complex formation on the vibrational spectra has been observed for the N−H stretching mode and the fingerprint region (N−H in plane bending modes). Several bands in the fingerprint region for the complex have been shown to be suitable indicator bands for detection of complex formation in polymer electrolytes where imidazole and imidazolium ions have been added.

Acknowledgment. This work has been supported by the European F95 IHP programme (research training network contact no. H9RN-CT-2000-19).

References and Notes

(1) Böddeker, K. W.; Peinemann, K.-V.; Nunes, S. P. *J. Membr. Sci*. **2001**, *185*, 1.
(2) Kreuer, K. D. *J. Membr. Sci*. **2001**, *185*, 29.
(3) Kreuer, K. D.; Fuchs, A.; Ise, M.; Spaeth, M.; Maier, J. *Electrochim. Acta* **1998**, *43*, 1281.
(4) Sun, J.; Jordan, L. R.; Forsyth, M.; MacFarlane, D. R. *Electrochim. Acta* **2001**, *46*, 1703.
(5) Münch, W.; Kreuer, K. D.; Silvestri, W.; Maier, J.; Seifert, G. *Solid State Ionics* **2001**, *145*, 437.
(6) Frisch, M. J.; Trucks, G. W.; Schlegel, H. B.; Scuseria, G. E.; Robb, M. A.; Cheeseman, J. R.; Zakrzewski, V. G.; Montgomery, J. A., Jr.; Stratmann, R. E.; Burant, J. C.; Dapprich, S.; Millam, J. M.; Daniels, A. D.; Kudin, K. N.; Strain, M. C.; Farkas, O.; Tomasi, J.; Barone, V.; Cossi, M.; Cammi, R.; Mennucci, B.; Pomelli, C.; Adamo, C.; Clifford, S.; Ochterski, J.; Petersson, G. A.; Ayala, P. Y.; Cui, Q.; Morokuma, K.; Malick, D. K.; Rabuck, A. D.; Raghavachari, K.; Foresman, J. B.; Cioslowski, J.; Ortiz, J. V.; Stefanov, B. B.; Liu, G.; Liashenko, A.; Piskorz, P.; Komaromi, I.; Gomperts, R.; Martin, R. L.; Fox, D. J.; Keith, T.; Al-Laham, M. A.; Peng, C. Y.; Nanayakkara, A.; Gonzalez, C.; Challacombe, M.; Gill, W.; Johnson, B.; Chen, W.; Wong, M. W.; Andres, J. L.; Gonzalez, C.; Head-Gordon, M.; Replogle, E. S.; Pople, J. A. *Gaussian 98*, revision A.6; Gaussian: Pittsburgh, PA, 1998.
(7) Dewar, M. J. S.; Zoebisch, E. G.; Healy, E. F.; Stewart, J. J. P. *J. Am. Chem. Soc*. **1985**, *107*, 3902.
(8) Christen, D.; Griffiths J. H.; Sheridan, J. *Z. Naturforsch*. **1982**, *37a*, 1378.
(9) Basch, H.; Krauss, M.; Stevens, W. J. *J. Am. Chem. Soc*. **1985**, *107*, 7267.
(10) Scheiner, S.; Yi, M. *J. Phys. Chem*. **1996**, *100*, 9235.
(11) Caswel, D. S.; Spiro, T. G. *J. Am. Chem. Soc*. **1986**, *108*, 6470.
(12) Perchard, C.; Bollocq, A. M.; Novak, A. *J. Chim. Phys*. **1965**, *62*, 1344.
(13) King, S. T. *J. Phys. Chem*. **1970**, *74*, 2133.
(14) Majoube, M. *Proceedings of the 6th International Conference on Raman Spectroscopy*; Heyden: London, 1978; Vol. 2, p 10.
(15) Colombo, L.; Bleckmann, P.; Schrader, B.; Plesser, T. *J. Chem. Phys*. **1974**, *61*, 3270.
(16) Salama, S.; Spiro, T. G. *J. Am. Chem. Soc*. **1978**, *100*, 1105.
(17) Majoube, M. *J. Mol. Struct*. **1980**, *61*, 129.
(18) Asher, S. A.; Murtaugh, J. L. *Appl. Spectrosc*. **1988**, *42*, 83.
(19) Majoube, M.; Henry, M.; Chinsky, L.; Turpin, P. Y. *Chem. Phys*. **1993**, *169*, 231.
(20) Sadlej, J.; Jaworski, A.; Miaskiewicz, K. *J. Mol. Struct*. **1992**, *274*, 247.
(21) Schwenke, D. W.; Truhlar, D. G. *J. Chem. Phys*. **1985**, *82*, 2418.
(22) Frisch, M. J.; Del Bene, J. E.; Binkley, J. S.; Schaefer, H. F. J., III. *Chem. Phys*. **1986**, *84*, 2279.